

Late-time Phase transition and the Galactic halo as a Bose Liquid: (II) the Effect of Visible Matter

S.U. Ji and S.J. Sin

Department of Physics, Hanyang University

Seoul, 133-791, Korea

(October 25, 2018)

Abstract

In the previous work, we investigated the rotation curves of galaxies assuming that the dark matter consists of ultra light boson appearing in 'late time phase transition' theory. Generalizing this work, we consider the effect of visible matter and classify the types of rotation curves as we vary the fraction of the mass and extension of visible matter. We show that visible matter, in galaxies with flat rotation curves, has mass fraction 2% \sim 10% and it is confined within the distance fraction 10% \sim 20%.

arXiv:hep-ph/9409267v1 10 Sep 1994

I. INTRODUCTION

Recently, motivated by the large scale structure, an ultra light Nambu-Goldstone boson was introduced in dark matter physics under the name of "late time cosmological phase transition" [1]. The basic idea of the theory is that if a phase transition happened *after* decoupling, one can avoid the constraint imposed by the isotropy of the microwave background.

Subsequently, one of the authors of this paper [2] tried to apply this idea to the rotation curve of galactic haloes. If the phase transition occurred so late, the universe was already big, therefore the relevant particle must be such that (i) its Compton wave length provides the scale of interest since there is no other length scale of this kind. (ii) it should be a major component of dark matter [3] to be responsible for the structure formation.

If the dark matter consists of this particle whose mass is, say, $m \sim 10^{-24}eV$ and if the dark matter density in the galaxy is about $10^{-25}g/cm^3$, then the inter particle distance is of order $10^{-13}cm$, while the Compton wave length is of 10pc order. Therefore the wave functions of the particles are entirely overlapping and a galactic halo is a giant system of a bose liquid. In this context, one must consider the dark matter distribution quantum mechanically and this is done in ref. [2].

However, there was a point that had to be clarified further in that work. All the rotation curves obtained there were slightly increasing. While this is consistent with most of the data [4], [5], there are a few galaxies whose rotation curves are decreasing. In fact, in [2], the effect of the visible matter was not properly considered. Although most of the mass of a galaxy is attributed to the dark matter, the shape of the rotation curve can depend on the mass profile of the visible matter, especially near the core of a galaxy. In this paper, we consider the effect of the visible matter to the shape of the rotation curve more carefully in the scheme of the ref. [2].

We briefly recapitulate the main idea of the paper [2]. The dark matter that is consist of ultra-light boson is in a condensation state. Usually bosons condense in the ground state,

because in atomic physics situation, matter is always coupled to electromagnetism (cooling) and this efficiently lower the energy of a system. In our case, however, it was shown [2] that there is no mechanism to reduce the total energy of the system, therefore we look for the non-ground state condensation described by a macroscopic wave function that has nodes. We will classify the rotation curves for three thousand different visible matter distributions.

II. QUANTUM FLUID OF DARK MATTER

The system is described by a macroscopic wave function (order-parameter) ψ . For simplicity, we consider spherically symmetric case. We also set the visible matter distribution to be spherically symmetric. This is not realistic, because the visible matter distribution of the disk galaxy is by definition not spherical. However, the purpose of this paper is to show the possibility of the decreasing curves and we believe that, for this purpose, it is enough to consider the spherically symmetric case only. We set the visible matter potential by hand and get the wave function of total system by numerical work. Also, we neglect inter-particle interactions apart from gravity. Since total distribution determines the potential of an individual particle, we expect that the system be described by a solution of non-linear rather than linear wave equation.

Newtonian potential V is given by

$$\nabla^2 V = 4\pi G(\rho_{dark} + \rho_{visible})$$

and the schrödinger equation is

$$i\hbar\partial_t\psi = -\frac{\hbar^2}{2m}\nabla^2\psi + V \cdot \psi(r) \quad (1)$$

By identifying $\rho_{dark} = GM_0m|\psi|^2$ and defining $\rho_{visible} = GM_0m\rho_v$ we get

$$i\hbar\partial_t\psi = -\frac{\hbar^2}{2m}\nabla^2\psi + GmM_0 \int_0^r dr' \frac{1}{r'^2} \int_0^{r'} dr'' 4\pi r''^2 (|\psi|^2 + \rho_v) \cdot \psi(r) \quad (2)$$

Here, M_0 is a mass parameter introduced for dimensional reason. We now set effective density of the visible matters as the Plummer potential for the bulge and exponential decay

for the disk. In eq. (1) it is important to remember that ψ describes the state of the whole system rather than a state of an individual particle. The justification of the non-relativistic treatment can be found in the ref. [2]. The basic idea is $v \sim GmM \sim 10^{-2}$, because in our case $M \sim 10^{12}M_\odot$ and $m \sim 10^{-24}eV$ as we shall see.

In this paper we consider two parameters that determine visible matter distribution. The one is the mass ratio of visible matter to dark matter and the other is the distance ratio of the distance in which 90% of visible matter exist to that in which 90% of dark matter exist.

Now we come back to the Eq.(1). It is non-linear, hence we do not have the freedom to normalize the solution. However, as shown in ref. [2] this equation has a scaling symmetry which allows us to resolve the ambiguity due to the choice of M_0 . That is, the physical quantity M does not depend on the choice of M_0 . We are interested in a stationary solution $\psi(r, t) = e^{-iEt/\hbar}\psi(r)$. We simplify the Eq.(1). After scaling by

$$r = r_0\hat{r}, \quad \psi = r_0^{-3/2}\hat{\psi}, \quad \rho_v = r_0^{-3}\hat{\rho}_v, \quad E = \frac{\hbar^2}{2m}\epsilon, \quad r_0 = \frac{\hbar^2}{2GM_0m^2}$$

We can write (1) in terms of the radial wave function $u(\hat{r})$.

$$\ddot{u}(\hat{r}) + \left(\epsilon - \int_0^{\hat{r}} d\hat{r}' \frac{1}{\hat{r}'} \int_0^{\hat{r}'} d\hat{r}'' (u^2(\hat{r}'') + \hat{\rho}_v(\hat{r}'')\hat{r}''^2) \right) \cdot u(\hat{r}) = 0 \quad (3)$$

where $\hat{\psi}(\hat{r}) = \frac{1}{\sqrt{4\pi}} \frac{u(\hat{r})}{\hat{r}}$. We solve this equation numerically.

III. SCALING ANALYSIS

In equation (2) there is a scaling symmetry. That is, the eq.(2) is invariant under the scaling

$$u \rightarrow \lambda u, \quad \hat{r} \rightarrow \lambda^{-1}\hat{r}, \quad \epsilon \rightarrow \lambda^2\epsilon, \quad \hat{\rho}_v \rightarrow \lambda^4\hat{\rho}_v. \quad (4)$$

Therefore, if $u(\hat{r}, \epsilon, \hat{\rho}_v)$ is a solution, so is $\lambda u(\lambda\hat{r}, \lambda^2\epsilon, \lambda^4\hat{\rho}_v)$. Let $\hat{M} = \hat{M}_{dark} + \hat{M}_{visible} = \int u^2 d\hat{r} + \int \hat{\rho}_v \hat{r}^2$. When we scale $\hat{r} \rightarrow \lambda^{-1}\hat{r}$, $\hat{M} \rightarrow \lambda\hat{M}$. Since $r = r_0\hat{r}$ is a physical quantity, it should be invariant under the scaling. Therefore $r_0 \rightarrow \lambda^{-1}r_0$. On the other hand, $r_0 \sim 1/(M_0m^2)$, hence $M_0m^2 \rightarrow \lambda M_0m^2$. The scaling of the normalized velocity \hat{v} can be

found as follows. The virial theorem tell us $v^2 = GM/r$, so $v = \sqrt{GM_0/r_0}\sqrt{\hat{M}/\hat{r}} := v_0 \cdot \hat{v}$. Therefore under the scaling above, we should get $v_0 \rightarrow \lambda^{-1}v_0$ to get physical velocity $v_0\hat{v}$. On the other hand, $v_0 \sim M_0m$. Hence we get $M_0m \rightarrow \lambda^{-1}M_0m$. Summarizing, under the scaling $\hat{r} \rightarrow \lambda^{-1}\hat{r}$,

$$\begin{aligned} M_0m^2 &\rightarrow \lambda^{-1}M_0m^2 \\ M_0m &\rightarrow \lambda^{-1}M_0m \end{aligned}$$

Therefore m is scaling invariant while $M_0 \rightarrow \lambda^{-1}M_0$. Consequently, $M = M_0 \cdot \hat{M}$ is scaling invariant as it should be.

Why did we do above analysis? In solving Eq.(2), we must choose the two initial values. The one is chosen $\hat{u}(0) = 0$, because $\hat{u}(r)$ is a radial wave function. In case of linear Schödinger equation, there is a freedom of normalization so that one can freely choose first derivative of u at $r = 0$, or $\psi(0)$. Here, the equation is non-linear and we do not have the freedom of normalization. We are in trouble unless something happens. It is the scaling symmetry we proved that save our trouble. In our numerical work, whichever we choose \hat{u}_0 or $\lambda\hat{u}_0$ as the initial value, the physical quantity is not changed. We set $\hat{u}(h) = 0.05 * h$, where h is a small segment of \hat{r} .

Now, we set the visible matter distribution as follows.

$$\hat{\rho}_v\hat{r} = \begin{cases} \hat{\rho}_0 \cdot \frac{1}{((\hat{r}/\hat{r}_d)^2+1)^{2.5}} & \text{for inner bulge} \\ \hat{\rho}_v(\hat{r}_d) \cdot e^{(\hat{r}_d-\hat{r})} & \text{for the disk} \end{cases}$$

We study for various values of ρ_0 and \hat{r}_d . We classify the rotation curve ($v(r)$) with the mass and the distance ratio of the visible matter to the dark matter.

IV. COMPARISON WITH OBSERVED DATA

Now we present the main result of this paper. We looked for solutions with 5 or 6 nodes. This choice is motivated partly because, in this state there is a rotation curve very similar to NGC2998, and NGC801. Additional reason is if we take node number bigger than 7,

the total mass of the halo is larger than $10^{13}M_{\odot}$. Hence there are some restrictions in our choice. Furthermore, in node number 4,3,2,1, the flat region is very narrow, and very hard to classify. So, we choose node number 5, and 6.

In figure-1, we compare NGC2998 and 5.6M–19.7D where 5.6M means the ratio of (visible matter mass) / (total mass) is 5.6% and 19.7D means (90% of visible matter dispersion distance) / (90% of total matter dispersion distance) is 19.7%. There are four ripples in the NGC2998's data. But we suspect that outside the measured region there might still be density peaks and nodes that could lead to further ripples. We can see that the shapes of measured and computed rotation curves are very similar except near the core of the galaxy, where the error of measured data is relatively big. By comparing the maximal velocity and the size of a ripple, we can get v_0 and r_0 . By using $m = \hbar/(\sqrt{2}r_0v_0)$ and $M_0 = r_0v_0^2/G$, we get $m = 2.90 \times 10^{-24}eV$ and $M_0 = 7.117 \times 10^{11}M_{\odot}$ in this case.

In figure-2, we compare NGC801 and 6.9M–12.7d. In this case $m = 3.14 \times 10^{-24}eV$ and $M_0 = 6.54 \times 10^{11}M_{\odot}$.

In the figures-3 and 4, Y axis is visible matter's 'mass ratio' to total mass, and X axis is 90% of the visible matter 'dispersion distance' to the total distance. The figures 3, 4 are the classification of the shapes of rotation curves. The symbol / means that corresponding rotation curve is increasing type, similarly \ means decreasing, and – means flat. When we measure a rotation curve in a real galaxy, we can't see full shape since we can observe only to the extent that sufficient amount of the hydrogen gas exists. So up, down, flat (/ , \ , –) classification is not for the full shape, but for the region that corresponds to first four or five ripples. The figures show that in a galaxy with relatively big visible mass ratio and small extension ratio has decreasing rotation curves, while the one with small mass ratio and large extension ratio has increasing data. This result is entirely consistent with the observation that compact bright galaxies have decreasing rotation curves and small dwarf galaxies have increasing rotation curves [8].

To give more intuition in reading the figures 3 and 4, we draw three rotation curves with the same mass ratio and different distance ratios. See figures 5, 6, 7, 8. We also give rotation

curves with the same distance ratio and different mass distance ratios.

Notice that we can find some interesting fact on the visible matter distribution from figures 3, 4. Our analysis shows that the flat region is confined in a small window, mass ratio 2% to 10 % and distance ratio 10% to 20%. On the other hand, the overall flatness is a general phenomenon in the real galaxies. Consequently, in our frame work, we can say that most galaxies, which have flat rotation curves, should have the mass and distance ratio in this range.

In figure 5, we fix the mass ratio $6.5\% \pm 0.5\%$, and change the rate of dispersion distance. Figure 6 is node 6 case. As we change the mass fraction of the visible matter, we can find three different types of rotation curve. With the change of the mass fraction, we can obtain various types of rotation curves. If the visible matter distribution is highly confined, the shape of the graph is of a decreasing form. When the visible matter distribution is widely dispersed, the graph is of slightly increasing a form that is very similar to the case of dark matter only. When its distribution is neither very dispersed nor very condense,

the graph is almost flat.

In the case shown in figures 5,6, the mass fraction of visible matter is not so large. So, the shape of the graph is not so different to the case of dark matter only. However, when the mass fraction of visible matter is very large, the situation is quite different. See figures 7, 8. In figure 7, we fix the mass ratio $25\% \pm 2\%$, and change the distance ratio in node 5. The same analysis for node 6 is shown in figure 8. Notice that in figures 7, 8 there is no flat curve in any case, and the shapes are quite different to the case of dark matter only.

In figure 9, we fix the distance ratio $12\% \pm 1\%$, and change the mass ratio node 5 case. Figure 10, is for node 6 case.

V. DISCUSSION AND CONCLUSION

In this paper we investigated the rotation curves of galaxies assuming that the dark matter consists of ultra light boson appearing in late time phase transition. Galactic halos

made of this species are highly correlated bose liquid. We develop a Landau-Ginzberg type theory describing the collective behavior of the system.

As the main results, we can obtain decreasing curves as well as flat and slightly increasing curves. In the previous work [2] we could see only slightly increasing curves, while observed data shows that a few galaxies have decreasing rotation curves. Here, we can see the flat curves and the decreasing curves as well by considering the visible matter, in addition to the dark matter. We show that the small amount of dark matter can change the shape of rotation curves near the core significantly.

Our paper has one interesting prediction. The flat case is confined in a rather small window corresponding to the mass ratio $2\% \sim 10\%$ and in the distance ratio $10\% \sim 20\%$. On the other hand of the observed galaxies has a 'flat rotation curve' So, we can predict that in most of galaxies have the mass ratio and distance ratio in that region.

So we conclude that the ultra light boson appearing in the late time phase transition theory has good enough properties to be a dark matter candidate, at least from the rotation curve point of view.

acknowledgement This work was supported by research fund of Hanyang University.

REFERENCES

- [1] C.T.Hill, D.N. Schramm, J. Fry, Comments of Nucl.& Part. Phys.**19**,25.
- [2] S.J.Sin, "Late time phase transition and the galactic halo as a bose liquid", preprint
- [3] J. Frieman, C. Hill and R. Watkins, Phys.Rev.D**46** 1226-1238 (1992)
- [4] V. Rubin et.al, Ap. J. **289** 81 (1985); Ap. J. **261** 439(1982); Ap. J. **238** 471 (1980).
- [5] V. Rubin in "Dark matter in the universe" by Kormendy and G.R. Knapp (eds.) IAU SYMP. **117**,(1985)
- [6] R. Ruffini and Bonazzola, Phys. Rev. **137** 1767(1969).
- [7] Landau and Lifshitz, Course of theoretical physics Vol.9 section 26.
- [8] Casertano and Alberta, in: *Baryonic Dark matter*, D. Lynden-Bell and Gilmore (eds.), NATO ASI Series C, Vol. 306
- [9] I. R. King, Astron. J. **71**64(1966).
- [10] Fukugita, Takasugi and Yosimura, Z. of Phys. C particles and Fields **27**,373-375(1985)
- [11] J. Binney and S. Tremaine, Galactic Dynamics, princeton univ. press
- [12] C.H. Lee and S.J. Sin, Quantum aspect of dark matter and star formation in elliptical galaxies, preprint HYUPT-93/07

FIGURES

FIG. 1. comparing the theory and observation for NGC2998 with the data that 5.6% of mass fraction and 19.7% of distance fraction

FIG. 2. comparing the theory and observation for NGC801 with the data that 6.9% of mass ratio and 12.7% of distance ratio

FIG. 3. classification of node 5 data; / means increasing, — means flat, \ means decreasing rotation curve

FIG. 4. classification of at node 6 data

FIG. 5. (1) mass ratio = 6.4% and distance ratio = 28.0%. (2) mass ratio = 6.3% and distance ratio = 13.0%. (3) mass ratio = 6.2% and distance ratio = 5.9%. AT node 5

FIG. 6. (1) mass ratio = 6.4% and distance ratio = 27.7%. (2) mass ratio = 6.3% and distance ratio = 13.6%. (3) mass ratio = 6.2% and distance ratio = 5.8%. At node 6

FIG. 7. (1) mass ratio = 25.4% and distance ratio = 27.4%. (2) mass ratio = 26.8% and distance ratio = 13.8%. (3) mass ratio = 26.8% and distance ratio = 5.9%. At node 5

FIG. 8. (1) mass ratio = 25.4% and distance ratio = 26.1%. (2) mass ratio = 25.8% and distance ratio = 14.3%. (3) mass ratio = 25.8% and distance ratio = 6.9%. At node 6

FIG. 9. (1) mass ratio = 0%. (2) mass ratio = 8.4% and distance ratio = 12.1%. (3) mass ratio = 14.6% and distance ratio = 12.8%. At node 5

FIG. 10. (1) mass ratio = 0%. (2) mass ratio = 8.4% and distance ratio = 12.2%. (3) mass ratio = 14.5% and distance ratio = 12.3%. At node 6

This figure "fig1-1.png" is available in "png" format from:

<http://arxiv.org/ps/hep-ph/9409267v1>

This figure "fig1-2.png" is available in "png" format from:

<http://arxiv.org/ps/hep-ph/9409267v1>

This figure "fig1-3.png" is available in "png" format from:

<http://arxiv.org/ps/hep-ph/9409267v1>

This figure "fig1-4.png" is available in "png" format from:

<http://arxiv.org/ps/hep-ph/9409267v1>

This figure "fig1-5.png" is available in "png" format from:

<http://arxiv.org/ps/hep-ph/9409267v1>

This figure "fig1-6.png" is available in "png" format from:

<http://arxiv.org/ps/hep-ph/9409267v1>

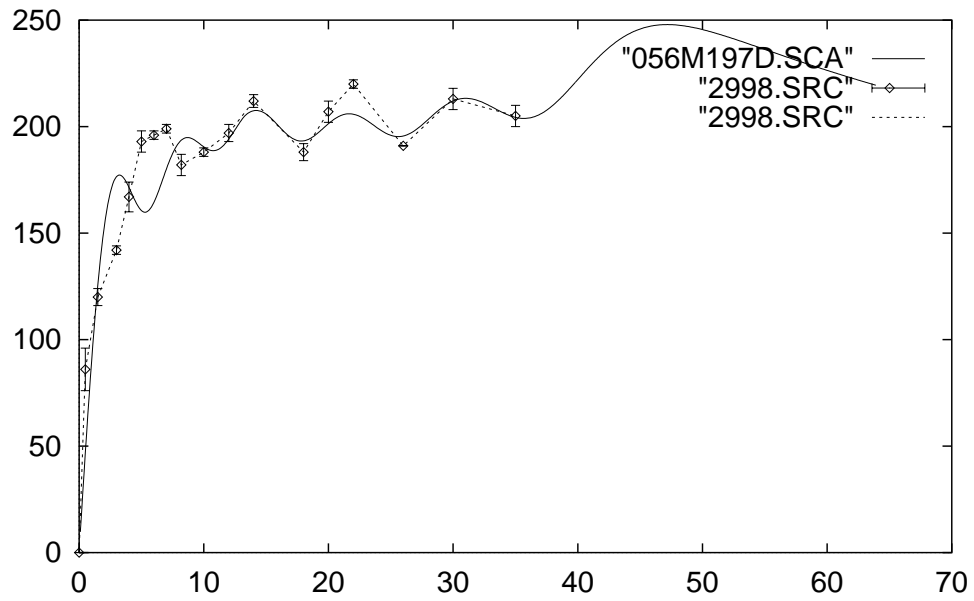


Figure 1

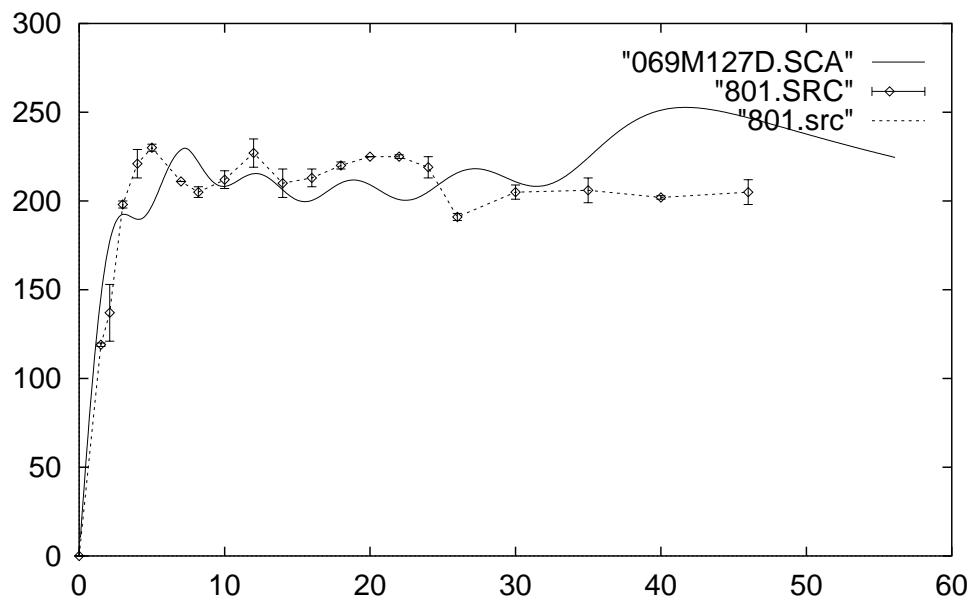


Figure 2

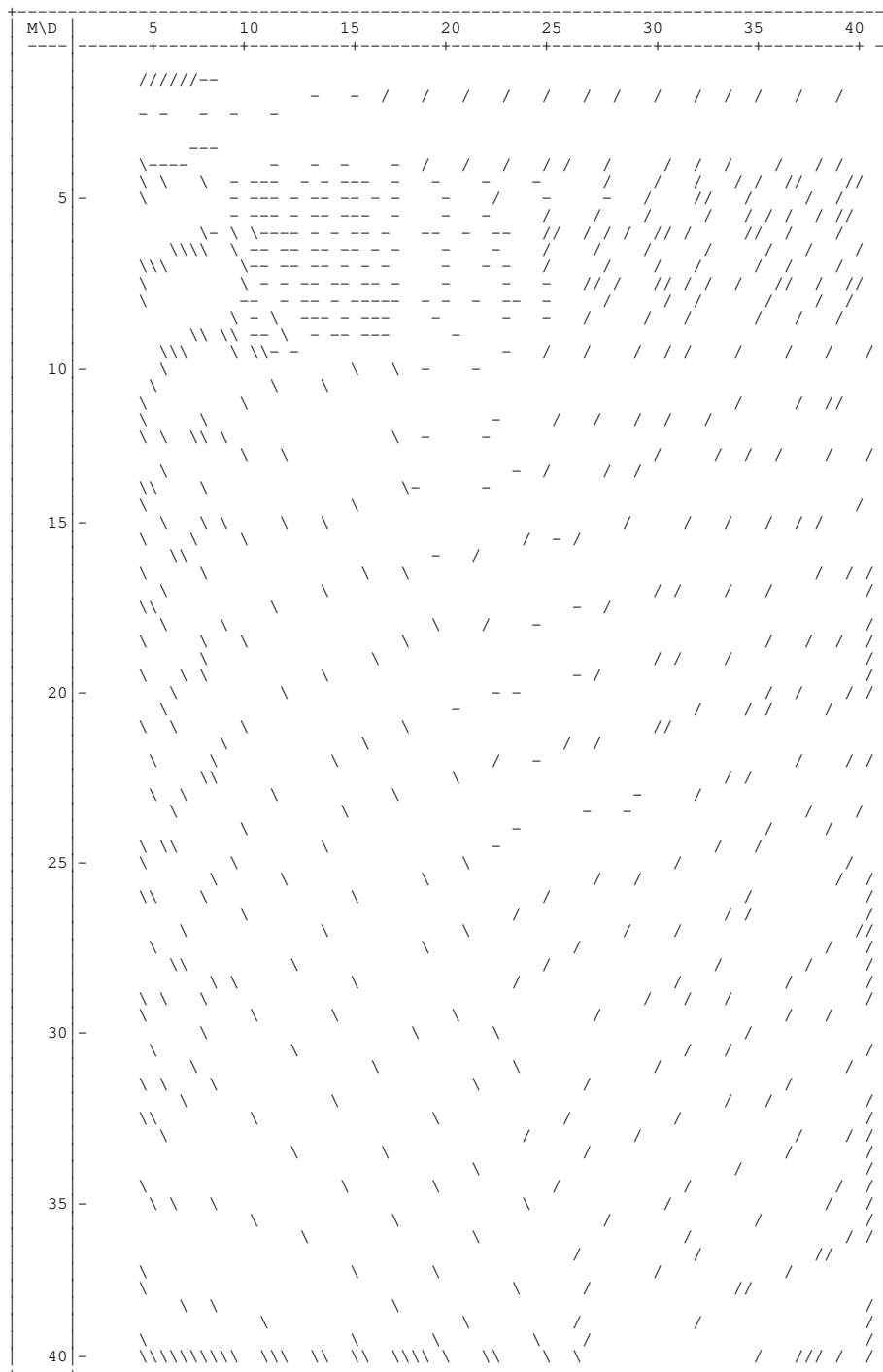
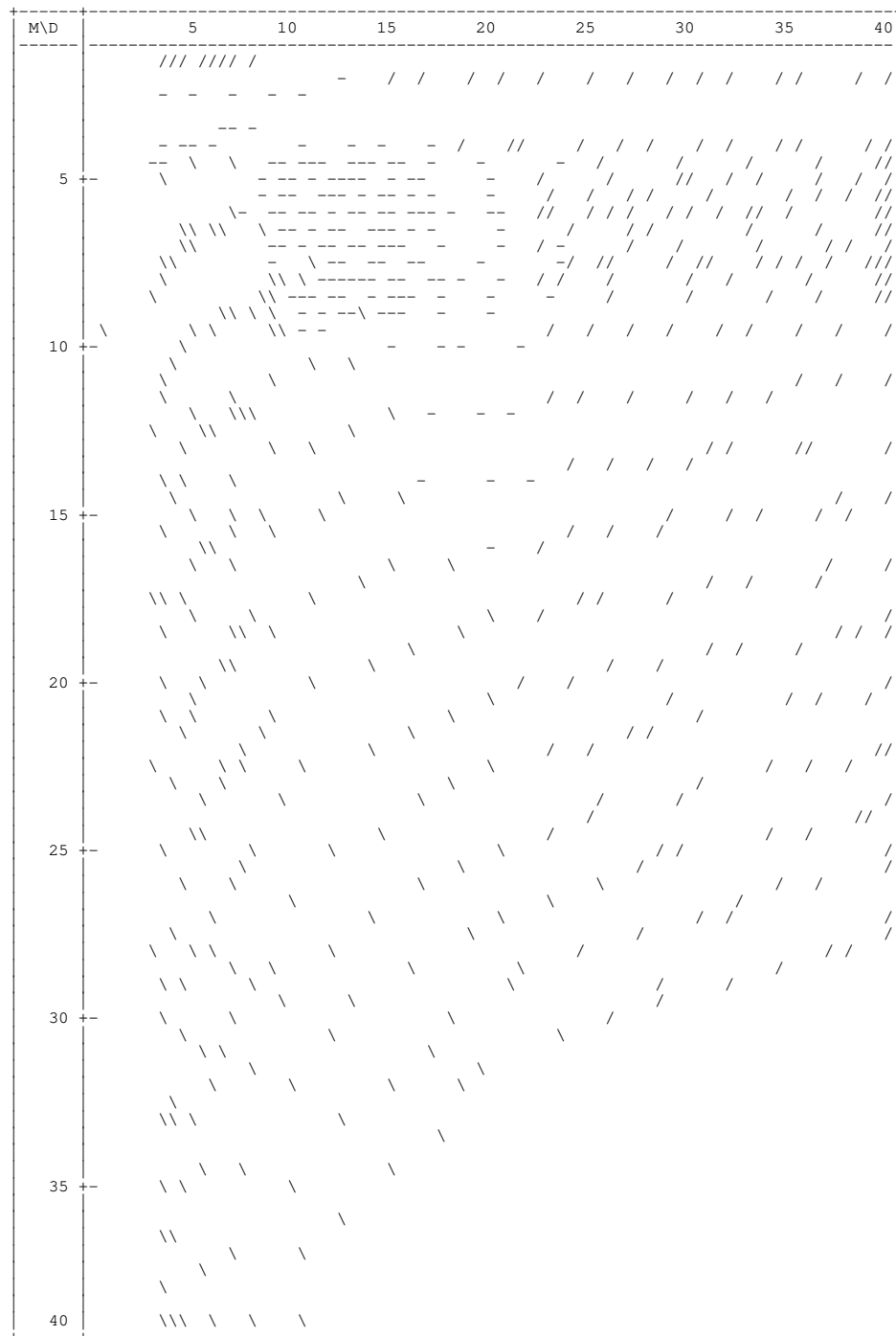


Figure 3



•@

Figure 4

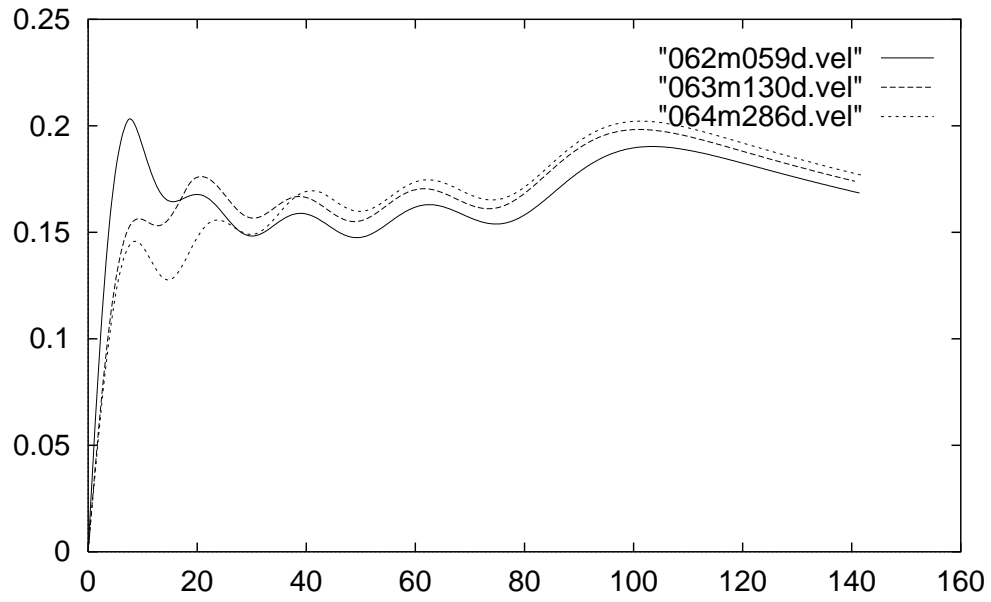


Figure 5

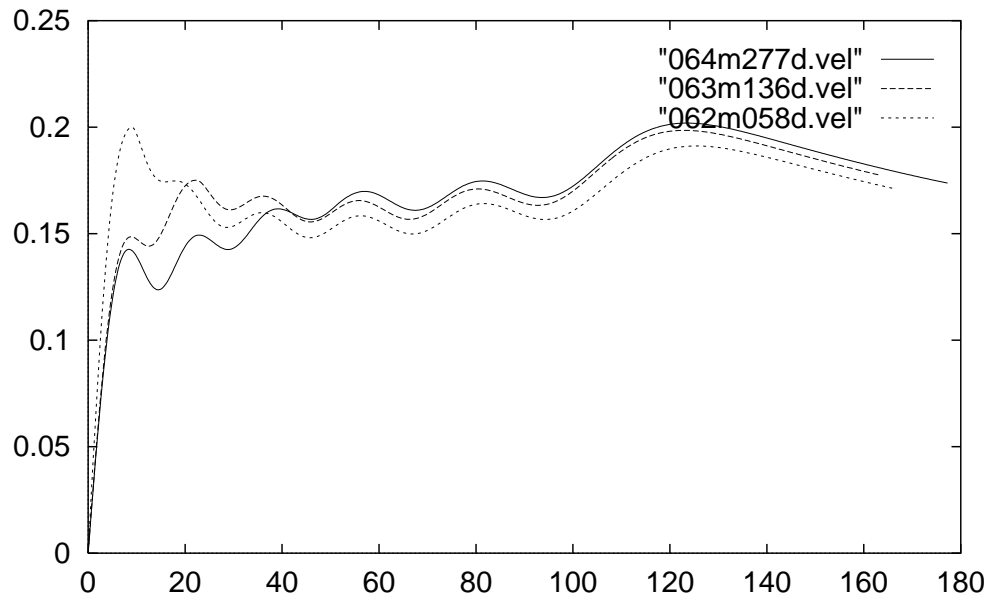


Figure 6

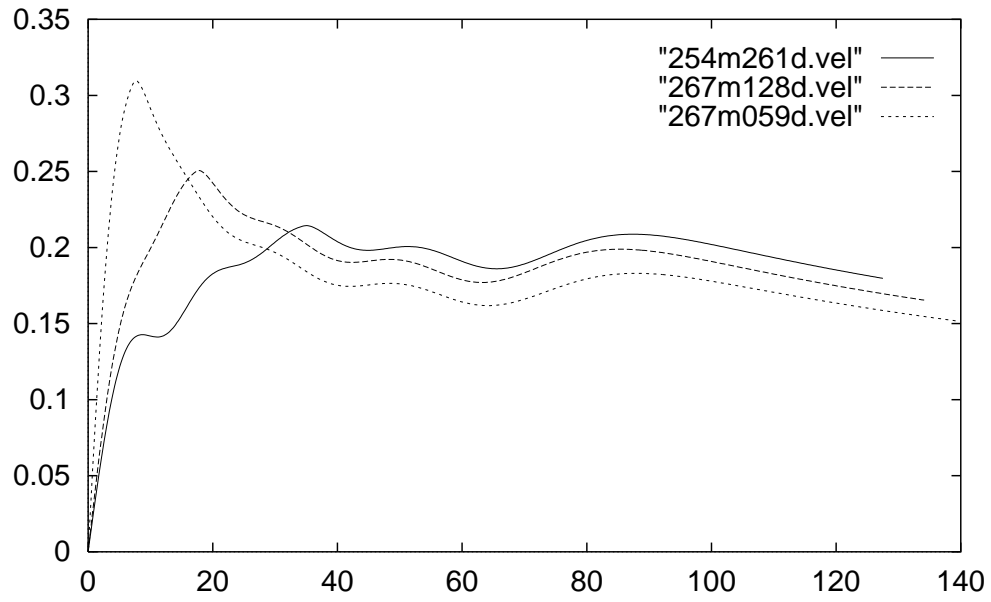


Figure 7

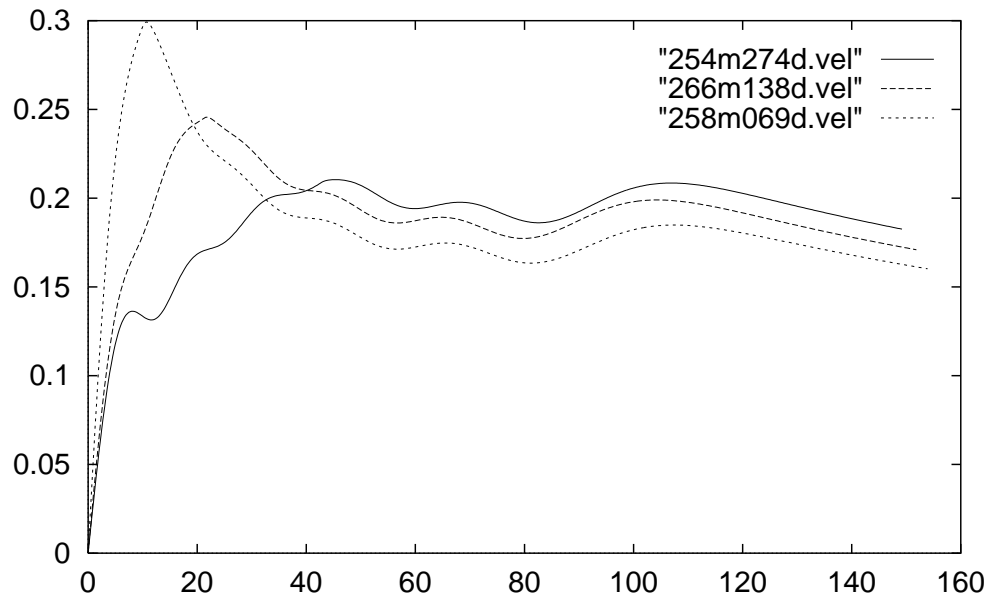


Figure 8

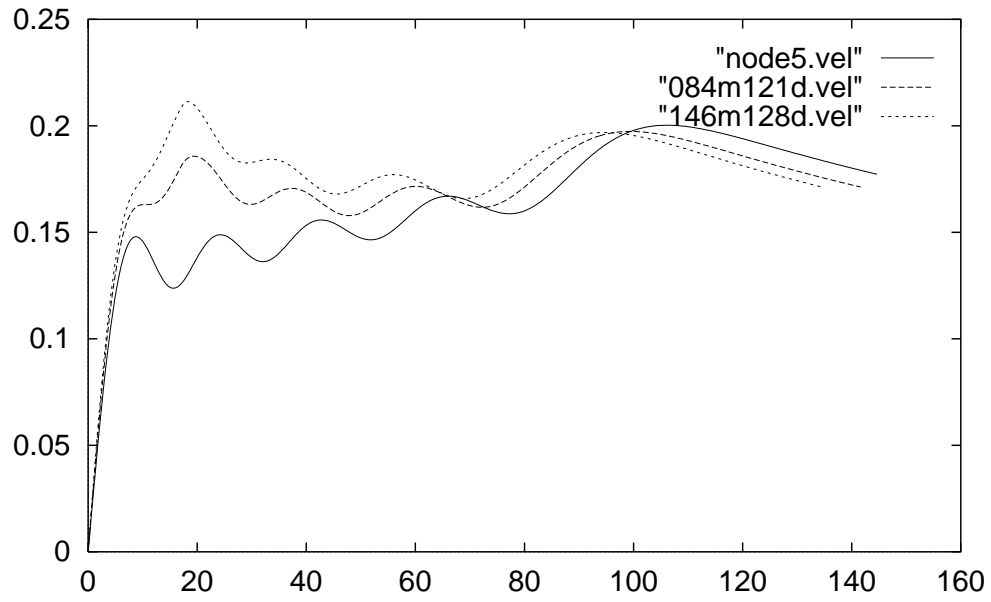


Figure 9

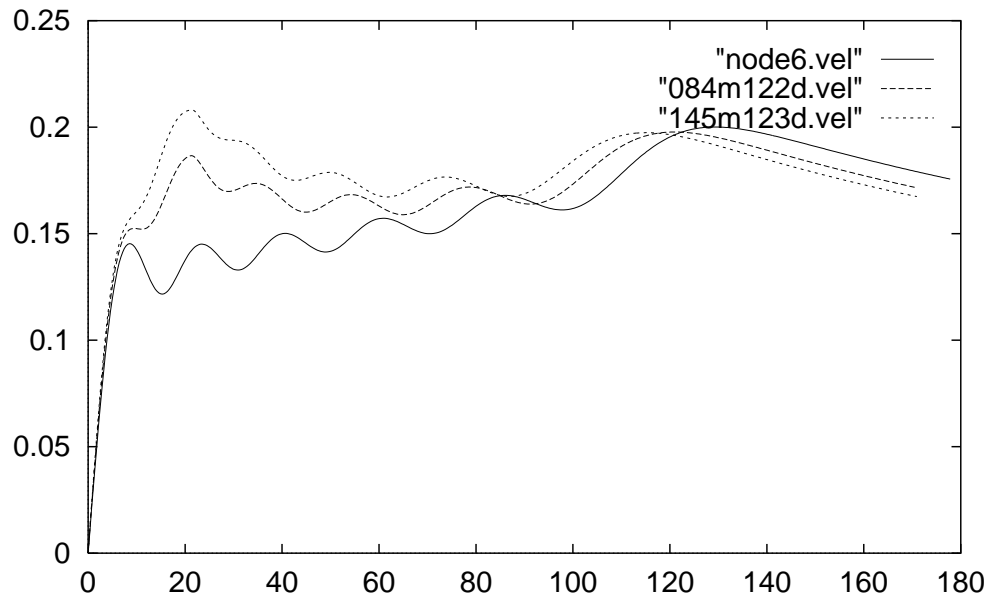


Figure 10